Top Fuel 2018. Prague, Czech Republic, 30 September – 04 October 2018

STAR-CCM+ SIMULATION OF A SPENT FUEL DRY CASK EXTERNAL COOLING BY NATURAL CONVECTION

Julio Benavides[1], Gonzalo Jimenez[1], Marta Galbán[2], Miriam Lloret[2]

[1] – Universidad Politécnica de Madrid - Spain

[2]- ENUSA Industrias Avanzadas S.A., S.M.E - Spain

As part of the nuclear industry moves towards dry storage systems, both in house and central storage systems, a renew interest in calculating peak cladding temperature, a key parameter for the cladding behaviour, has risen. In order to calculate the thermal performance of the dry cask a CFD calculation is usually employed to obtain the rod temperatures distribution mapwhere the inner part of the cask is modelled in detail. To get reliable results, the simulation should have realistic boundary conditions but traditionally a simple correlation is used to calculate the outside heat transfer coefficient.

In this paper we propose a new methodology that starts with an outside simulation of the container, as a first step to set up the inner cask boundary conditions. With this new approach, a surface specific heat transfer coefficient is calculated without the need of a correlation, as an additional output, these simulations have also allowed us to see the impact of the container in the environment (concrete basement and surrounding air). To ensure the correctness of the model several sensibility analysis have been performed including a grid convergence index study, a study of the impact of the fluid region simulated and a turbulence model sensibility analysis.

1. Introduction

As part of the nuclear industry moves towards dry storage system, a deeper interest for realistic calculation of cladding temperature in dry storage has risen. Radial hydride in claddings degrades the ductility under circumferential stress, to prevent this, maximum peak cladding temperatures must not exceed 400ºC [1]. Therefore calculating PCT (Peak Cladding Temperature) in a more realistic way becomes a necessity. In this paper a first step towards a new methodology in calculating peak cladding temperature is presented.

When a CFD calculation of the peak cladding temperature inside of a spent fuel dry cask is performed, some of the most influential parameters are the external boundary conditions of the cask i.e the air temperature distribution and the speed of the surrounding air. These variables are necessary to calculate the outside heat transfer coefficient.

In some of the cases in the public literature [2] the external boundary conditions are set using the Churchill and Chu correlation [3] (Equation [3]) for vertical surfaces (applied to the lateral part of the cask) and the W.H McAdams [4] for the horizontal plate (Equation [4]) (applied to the upper part of the cask). In some other works found in the literature, the temperature is set with a profile [5] or with a fix value for the heat transfer coefficient [6]–[8]

$$Nu_V = \left\{ 0.825 + \frac{0.387 Ra^{\frac{1}{6}}}{\left[1+\left(\frac{0.492}{Pr}\right)^{\frac{9}{16}}\right]^{\frac{8}{27}}} \right\}^2 \quad [1]$$

$$Nu_H = 0.15 Ra_L^{\frac{1}{3}} \ (10^7 \leq Ra_L \leq 10^{11} \quad [2]$$

Where Ra is the Rayleigh number and Pr is the Prandtl number as define in equation [5-6]

Although both correlations are easy to use and extremely useful when no other data is available, the applicability of them to a dry cask geometry is questionable. In this paper, the first step towards a new methodology is presented. This methodology is designed to achieve realistic values for temperature distribution throughout the cask life span using a CFD code. The first step consists of calculating the outside part of the cask in an open air room. This ensures the boundary conditions to be realistic and not based on a fix heat transfer coefficient or a temperature profile.

The next step, to be taken in a near future, will tackle the simulation of the inside of the cask, and different sensitivity analysis. To perform these simulations STAR-CCM+ 13.02 CFD code is employed. The TN-24P cask was chosen due to the extensive literature available, for instance the data obtained during the testing performed by EPRI [9] and the published research [5], [6], [10].

2. Computational Model

As stated before, in this first step a simulation of the outside of the cask is performed, to obtain the environmental impact that the cask has in the near environment. The idea is to obtain the most accurate results for the boundary conditions for the next step (a full scope simulation of the TN-24P inner part).

In order to get the most accurate results, the simulation replicates the experiment conditions [9]. Unfortunately, there are some unknowns regarding the disposition of the cask inside the warm shop (where the experiment was conducted), and other geometry factors.

The cask is modelled from the inside of the steel cylinder. The basket and fuel assemblies are not modelled, and the heat flux is imposed in the interior surface of the cylinder in the way summarized in *Table 1*. This heat flux distribution is one of the main hypothesis based on previous works conducted by [5], [6], [9] , and to be updated with the cask inner simulation.

	Percentage of heat output
Lateral cylinder	92%
Top lid	6%
Lower lid	2%

Table 1. Heat flux distribution [5], [6], [9]

The computational domain includes the cask solid material an open box of air, and the floor where the cask is sitting on, as can be seen onFigure 1. The lateral faces bounding the box of air are simulated as stagnation inlets whereas the top is simulated as a pressure outlet, this allows the air to move freely, the inlet and pressure outlet temperature is 293K and the pressure is kept as atmospheric pressure (101325 Pa). Since the room [9] where the experiment took place is large enough, the expected flow is buoyancy driven. The sides of the floor are adiabatic and the inferior plate is at a constant temperature of 288 K. To verify that the chosen simulation domain was adequate, a simulation with the complete room was done (24x15x15 m). The results are almost identical to that of the smaller domain (maximum temperature difference below 4ºC), therefore the smaller domain will be considered to be adequate.

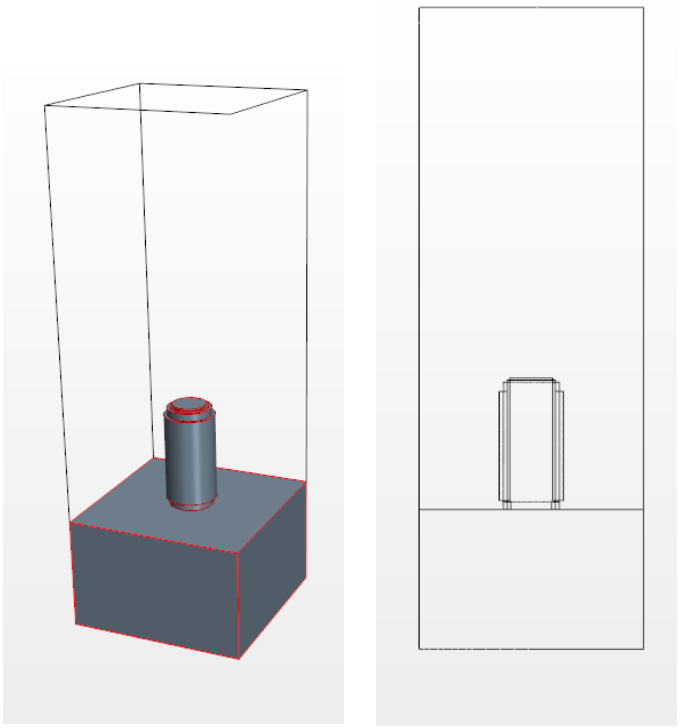

Figure 1. Geometry simulated and cross section

The numerical model and physics setting is summarized in *Table 2*. In the peer review process of the paper, a sensibility analysis was asked regarding the turbulence modelling employed, in particular four additional model were asked for (AKN k-ε, Standard Low Reynolds k- ε, Realizable k- ε (but shear driven instead of buoyancy driven), and v-2f k- ε). The results showed that the new models provide more accurate results, therefore some of the results have been recalculated and compared to the previous one. Unfortunately the GCI couldn't be recalculated due to time constraints and it will be done in future work for the other models.

Pressure-velocity coupling	Coupled Flow and Energy
Discretization	2nd Order
Temporal discretization	Steady State
Gas model	Ideal Gas
Turbulence model	K- ε Realizable (Buoyancy Driven) and Standard Low Reynolds k- ε
Wall Treatment	Two Layer All y+ Wall Treatment
Radiation	S2S
Density reference	1.21541 Kg/m^3

Table 2. Physics and numerical scheme

The air thermal conductivity and viscosity are variable with temperature [11], as for the solids only the constant thermal properties were available from the public information (and the exact nature of the materials unknown), therefore only constant values where employed (for the thermal conductivity, density and thermal capacity), nonetheless the solids are coupled to the fluids in the energy equation and participate in radiation exchange.

In order to understand what type of convection the model is obtaining an estimation of the ratio (Gr/Re^2) between the Grashof number and the Reynolds number, also known as the Richardson number, has been calculated. A value greater than 1 would indicate that forced convection may be ignore, whereas lower than one the free convection may be ignored, when the result is close to unity a mixed convection regime is to be expected. In this case the value is 8, therefore mixed convection.

$$Gr = \frac{L^3 \rho^2 g \Delta T \beta}{\mu^2}$$ Equation [3]

$$Re = \frac{\rho L v}{\mu}$$ Equation [4]

$$Ra_x = \frac{g \beta \Delta T x^3}{\alpha \upsilon}$$ Equation [5]

$$Pr = \frac{\upsilon}{\alpha}$$ Equation [6]

Where L is the main dimension, ρ is the fluid density, g is the gravity acceleration, ∆T if the temperature between the fluid and the surface, β is the thermal expansion coefficient, μ is the cinematic viscosity, v is the velocity of the fluid, α is the thermal diffusivity and υ is the kinematic viscosity.

One of the most important procedures when making a CFD analysis is conducting a meshindependence study. This step ensures that the discretization error is known and that it can be quantifiable. In particular, the methodology used is GCI or Grid Convergence Index, developed by Roache [12]. In this methodology, three meshes with different number of nodes are selected to conduct the study. The three meshes used for this case are described in Table 3. The chosen variable of interest is the maximum temperature in the lateral sides of the cask and the top lid, due to the importance to calculate the heat transfer in this study. To conduct the study the equations [3] through [6] are employed. The results in the top lid of the cask are

slightly worse than those obtained in the lateral surfaces, this is explained by the higher turbulence on top of the lid, which makes difficult to reach convergence criteria [13].

$$p = ln\left(\frac{f_3 - f_2}{f_2 - f_1}\right) / \ln(r)$$ Equation [7]

Where "p" is the observed order of convergence, "f_i" is the value of the studied variable for each mesh (f1 for the finer mesh and f3 for the coarser mesh), and "r" the ratio between meshes in this case r=2.27.

$$\varepsilon = \frac{f_2 - f_1}{f_1}$$ Equation [8]

$$GCI_{fine} = \frac{F_s|\epsilon|}{(r^p - 1)}$$ Equation [9]

$$GCI_{coarse} = \frac{F_s|\epsilon|r^p}{(r^p - 1)}$$ Equation [10]

F_s is a safety factor, it is recommended Fs=3 when only two meshes are employed and F_s=1.25 when three meshes are used (as is the case in this paper).

As can be seen in Table 4 the results for the fine mesh are very good in both regions therefore the results presented here, and for future studies will be done using the fine mesh.

Mesh	Number of cells
Coarse (3)	2.463.122
Fine (2)	5.586.033
Very fine (1)	12.827.695

Table 3. Meshes employed

Region	GCI2-3 (100%)	GCI1-2 (100%)
Neutron Shield surface	0.301135	0.093
Top lid	1.0771	2.1505

Table 4. GCI

3. Results

The two main results to study are the outside temperature distribution and the heat transfer coefficients in the outer part of the cask due to the results obtained during the peer review process the results below are a comparison between two of the models the Realizable k-ε (buoyancy driven) and Standard k-ε Low Reynolds. Unfortunately only the temperatures were measured, therefore the heat transfer coefficient obtained cannot be validated,

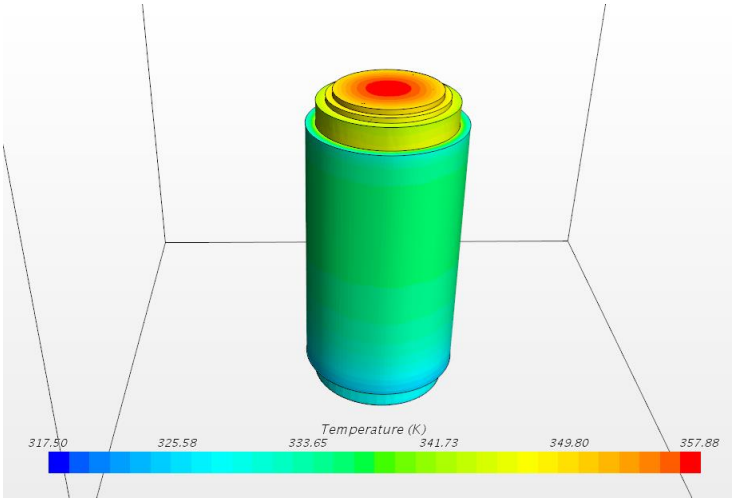

Figure 2. Outside cask surface temperatures (k-ε Realizable, Shear Driven)

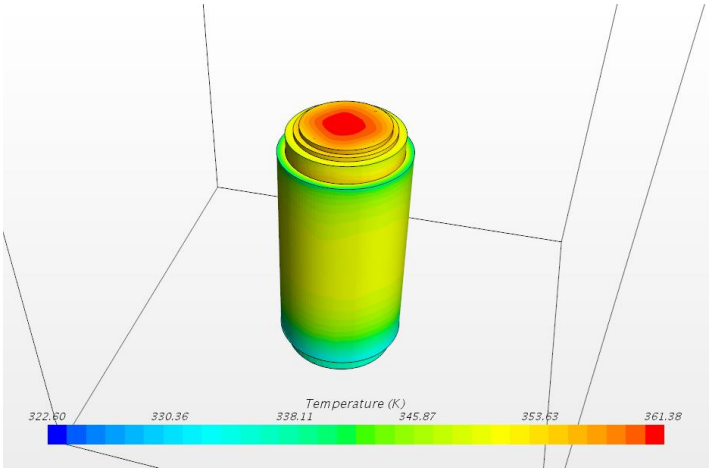

Figure 3. Outside cask surface temperatures (Standard k- ε Low Reynolds)

The simulation results vs the experimental results are shown inFigure 4. As can be seen the results are in good agreement with the experimental ones and are dependent on the turbulence modelled employed. It is clear that the Realizable k- ε (buoyancy driven) model is the least accurate and under-predicts the overall temperatures, whereas the rest of the models can predict the peak temperature and overall shape of the temperature distribution.

As for the top lid of the canister Figure 5, both the Realizable k- ε (buoyancy driven) and the Standard k- ε Low Reynolds are predicting both the maximum temperature and temperature distribution. The rest of the models are over predicting temperature trough out the region.

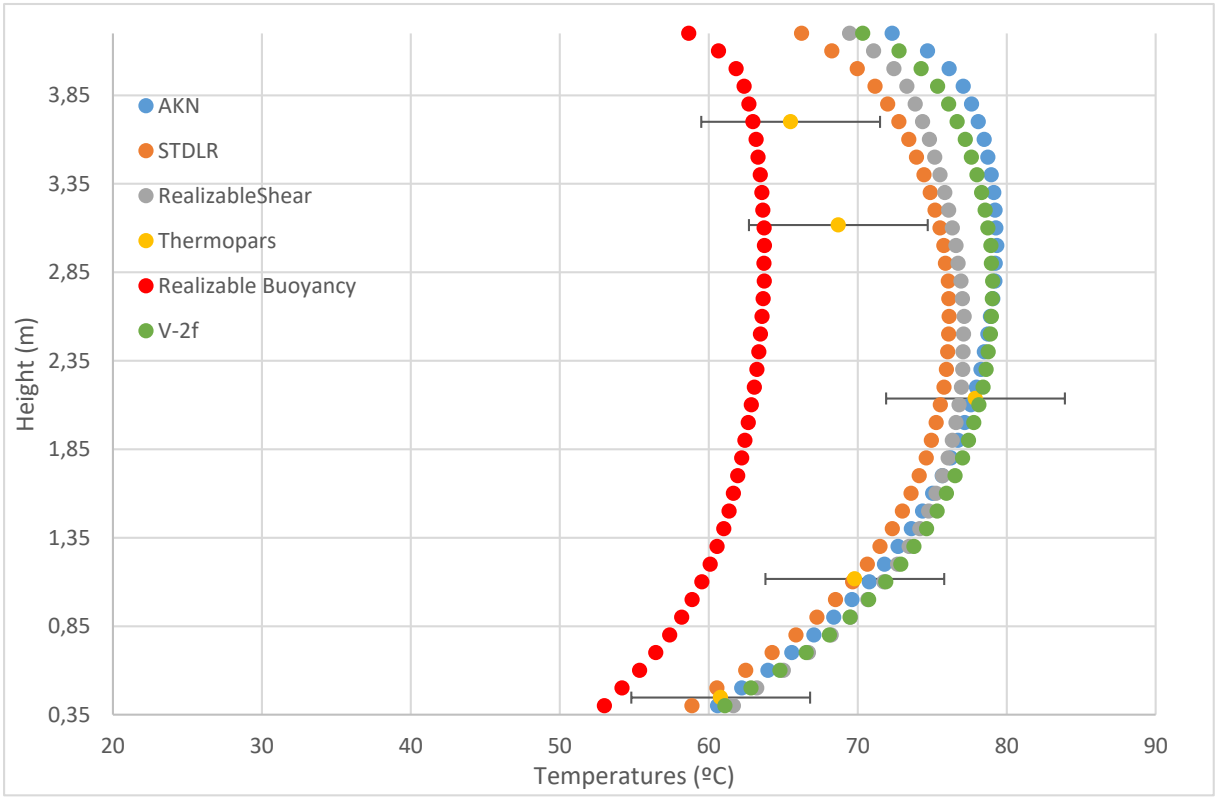

Figure 4. Lateral temperatures

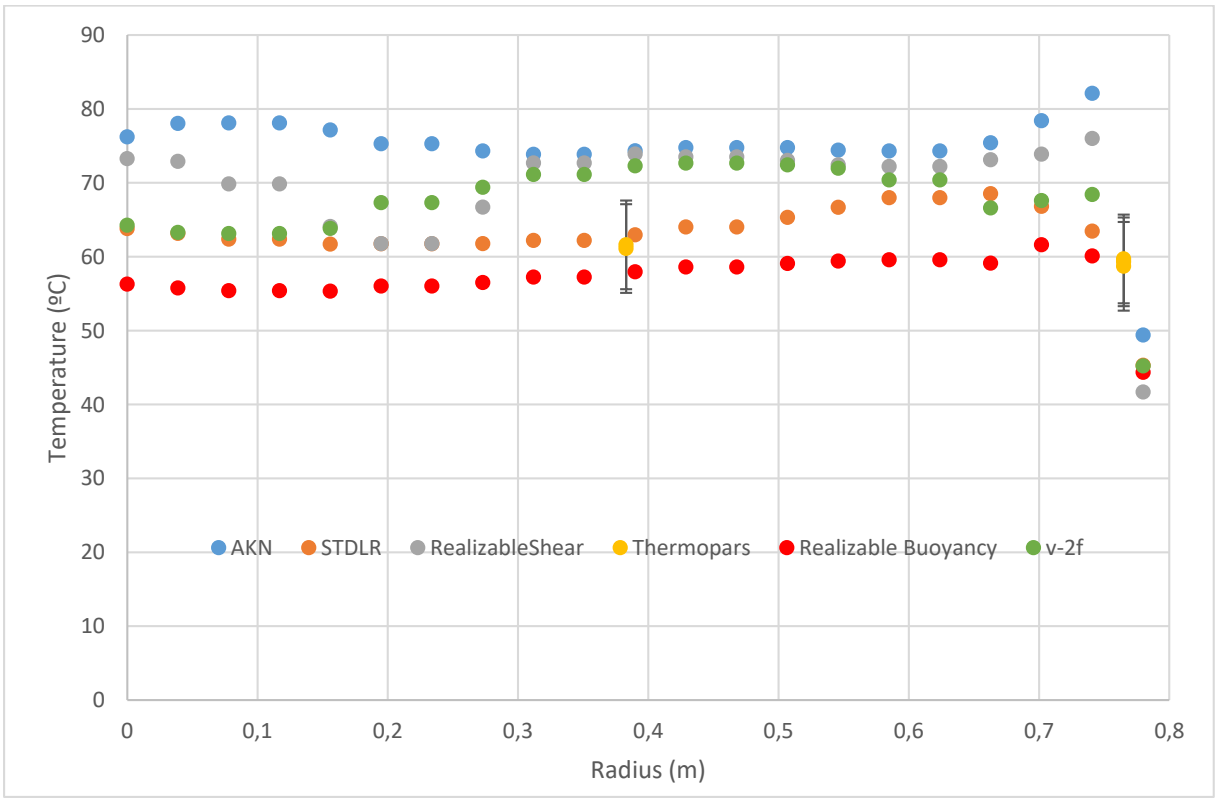

Figure 5.Top lid temperatures

Unfortunately no temperature distribution was provided for the bottom of the cask, therefore the temperature distribution obtained in the simulation is the only way to know what happened below the cask. To visualize the temperature on the upper surfaces of the cement Figure 6 and Figure 7 are provided, as can be observed the radial temperature gradient is quite large in both cases, meaning thermal degradation of the cement might be problematic. The maximum temperature is 66ºC for the Realizable k- ε (buoyancy driven) and 56ºC for the Standard k- ε Low Reynolds ºC in the contact between the bottom lid and the floor. Although the maximum temperature in the floor is relatively low in both cases, there is still an impact worth considering, especially in newer casks, which usually hold higher burn up fuel therefore higher temperatures are expected. In Figure 8 the temperature distribution on the centre line below the cask is shown.

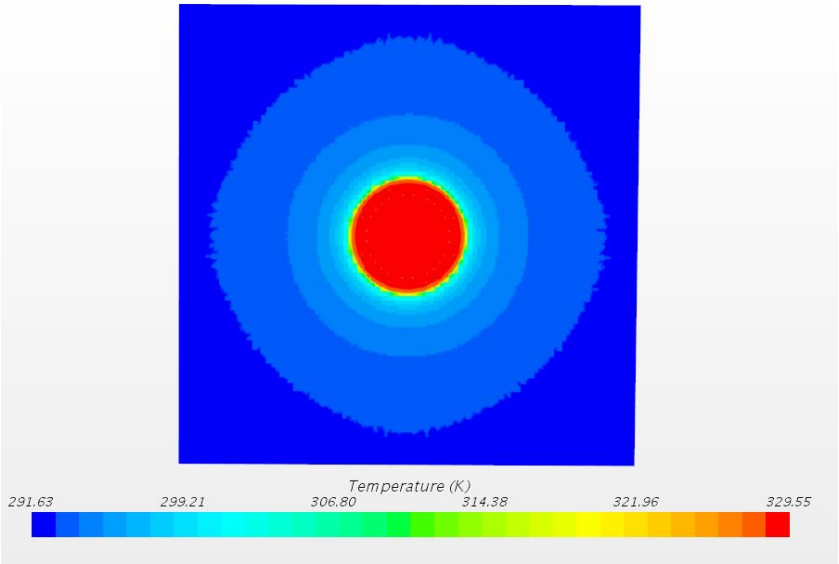

Figure 6. Temperature profile on the upper surface of the cement (k-ε Realizable, Buoyancy Driven)

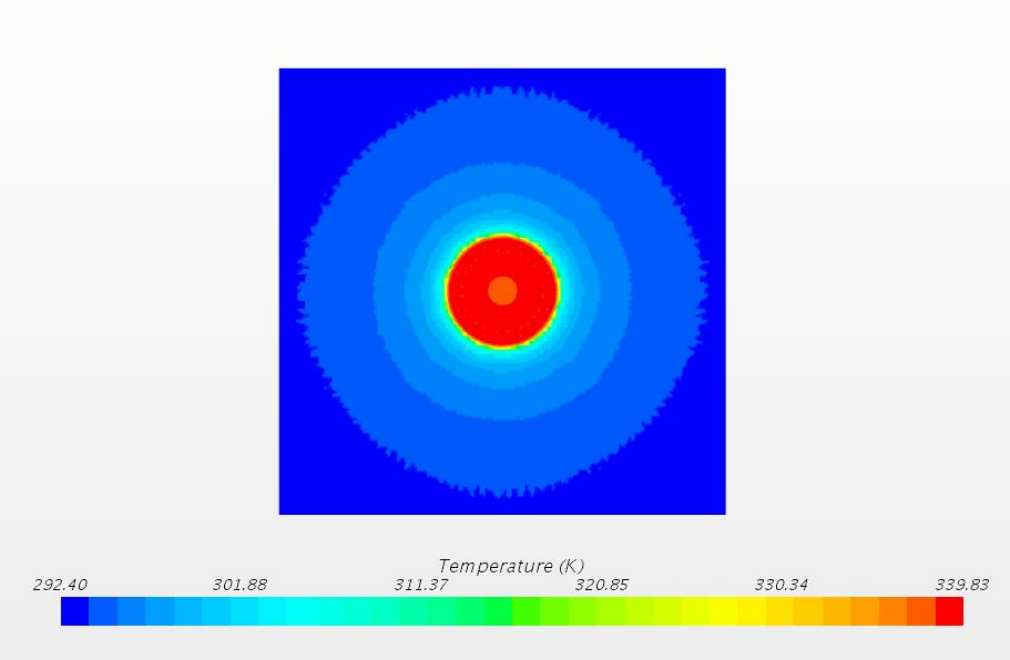

Figure 7.Temperature profile on the upper surface of the cement (Standard k-ε Low Reynolds)

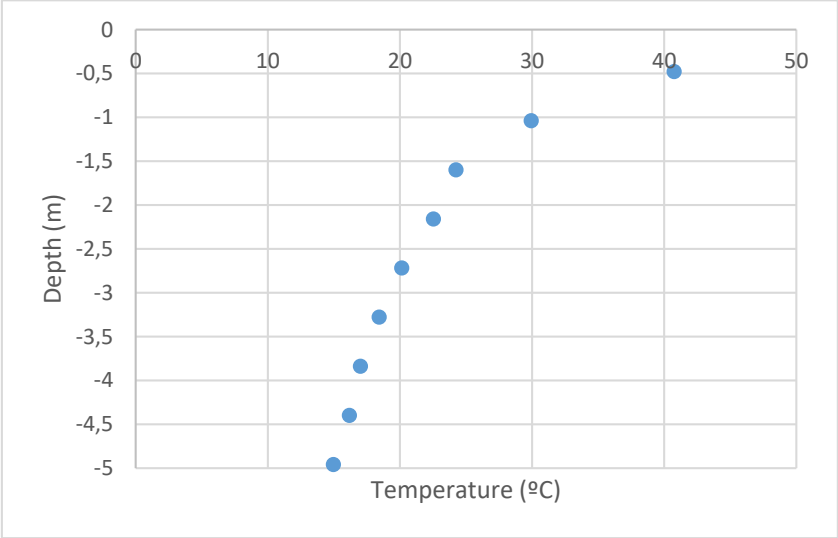

Figure 8. Temperature in the concrete floor.

In Figure 9, both the analytical heat transfer coefficient (Eq. [1]) and the simulated ones are presented for the whole surface of the neutron shield both vertical and horizontal surfaces. The vertical lines at the upper and lower parts of the graph are due to the horizontal surfaces of the neutron shield (constant height but different heat transfer coefficient).

There is a noticeable difference between the two turbulence models, where the Standard k- ε Low Reynolds agrees with the calculated value for most of the geometry, the Realizable k- ε (Buoyancy Driven) greatly differs both from the calculated and the other simulation.

Considering that the most accurate (Figure 4) is the Standard k- ε Low Reynolds, it is likely that the heat transfer coefficient taken from this simulation is the better of the two. Therefore it seems that the calculated value is better than initially thought and can capture the overall value of the heat transfer coefficient in the central regions of the cask; the upper and lower parts of the neutron shield (near the edges of the upper and lower part of the cask) are more complex and the calculated value is not as precise.

As for the top lid heat transfer coefficient (Figure 10), each model presents very different behaviour, where Realizable k- ε (Buoyancy Driven) presents not only higher value but also a more constant behaviour. The Standard k- ε Low Reynolds presents a very different behaviour, considerably less constant, higher in the centre of the lid, a decrease in the middle and a rapid increase near the edge. This clearly shows that complex geometries are not as easy to predict with a simple correlation. In either case the calculated value cannot represent such behaviour.

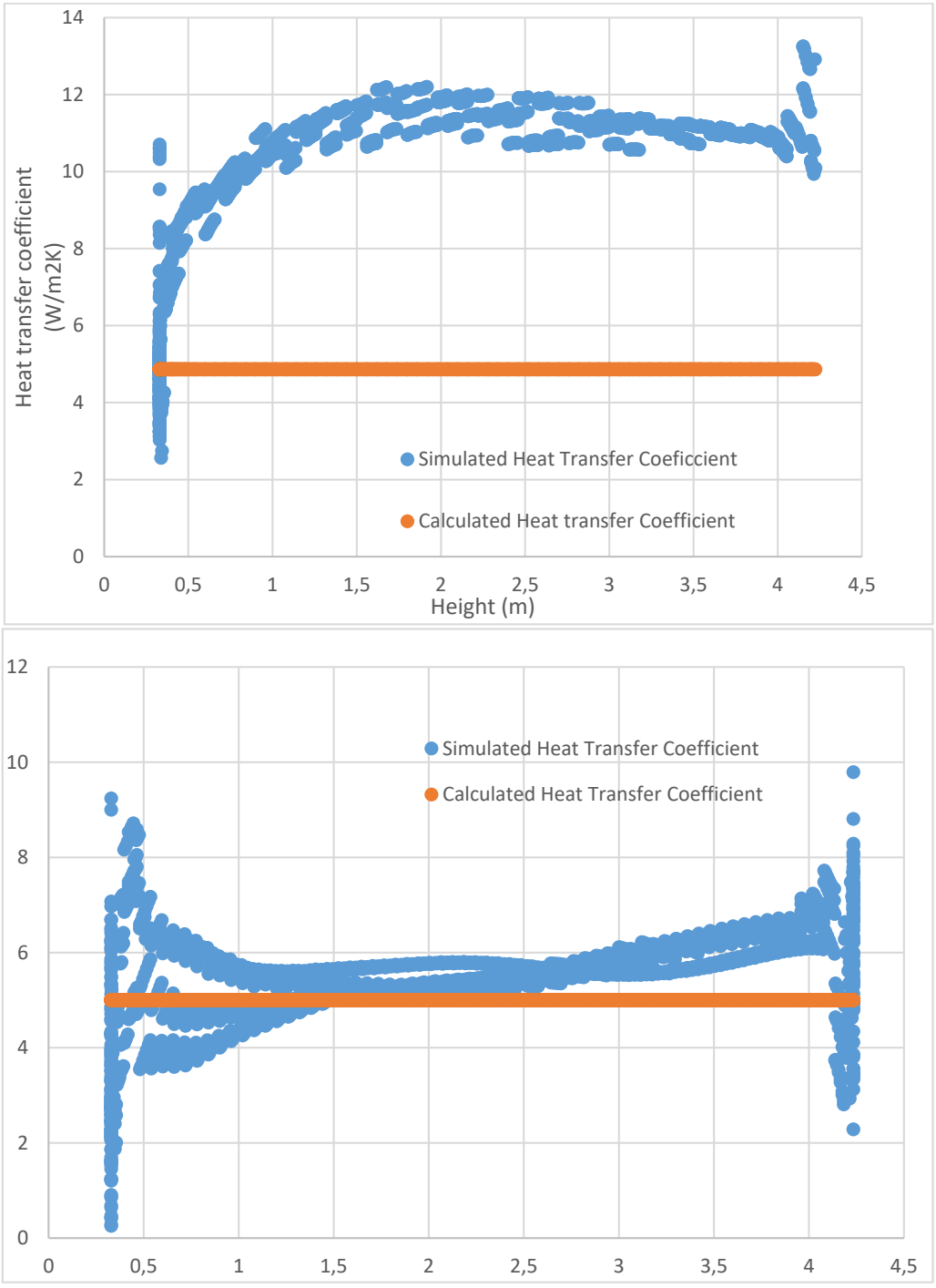

Figure 9 Heat transfer coefficient simulated and calculated. (Upper graph for k- ε Realizable (Buoyancy driven), Lower for Standard k- ε Low Reynolds)

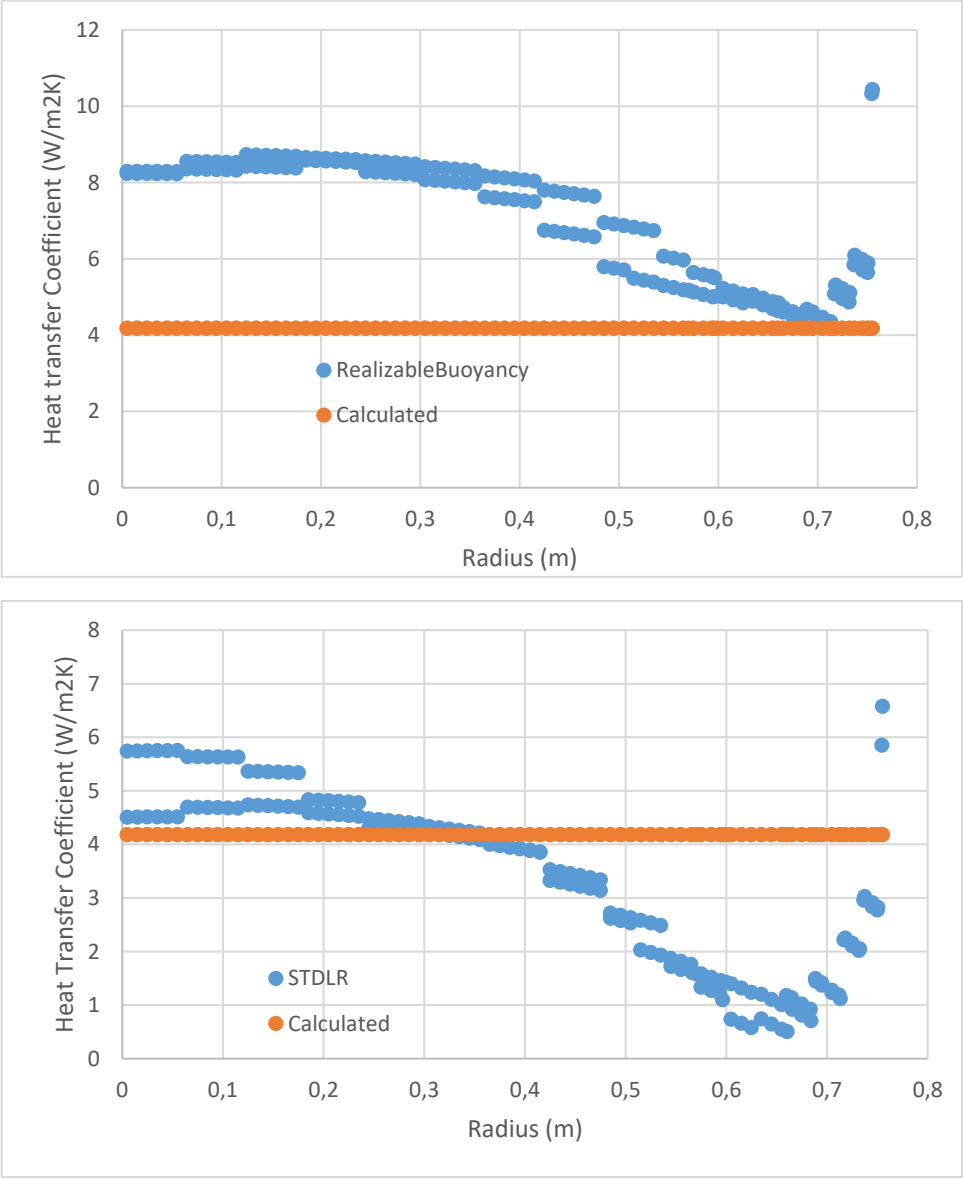

Figure 10. Heat transfer coefficient on the top lid (upper graph for Realizable k- ε Buoyancy Driven, and lower for Standard k- ε Low Reynolds).

4. Conclusions

A successful study of the outside of the cask has been performed, the results are in good agreement with the experimental ones it also illustrates the impact of different turbulence models have in both temperature distribution and heat transfer coefficient. It seems that the Standard k-ε Low Reynolds obtained the best results overall.

The heat transfer coefficient obtained has shown that the correlation seems to be an adequate way to calculate the heat transfer coefficient for the lateral walls, when the geometry is more complicated such as the edges or the top lid, the correlations are not as robust.

The next step in the methodology is the simulation of the cask inner part, since predicting peak cladding temperatures and temperatures distribution in a realistic manner is the most important factor in this new methodology. Several questions have to be answered when modelling the inside of the cask and will be faced in future works.

References:

[1] USNRC, «Spent Fuel Project Office, Interim Staff Guidance Nº 11, Revision 3». 2003.

[2] L. E. Herranz, J. Penalva, y F. Feria, «CFD analysis of a cask for spent fuel dry storage: Model fundamentals and sensitivity studies», *Ann. Nucl. Energy*, vol. 76, pp. 54–62, 2015.

[3] S. W. Churchill y H. H. S. Chu, «Correlating equations for laminar and turbulent free convection from a vertical plate», *Int. J. Heat Mass Transf.*, vol. 18, n.º 11, pp. 1323-1329, nov. 1975.

[4] McAdams, William H., «Heat Transmission (3d ed)». McGraw-Hill, 1954.

[5] S. H. Yoo, H. C. No, H. M. Kim, y E. H. Lee, «Full-scope simulation of a dry storage cask using computational fluid dynamics», *Nucl. Eng. Des.*, vol. 240, n.º 12, pp. 4111–4122, 2010.

[6] R. A. Brewster, E. Baglietto, E. Volpenhein, y C. S. Bajwa, «CFD analyses of the TN-24P PWR spent fuel storage cask», *Am. Soc. Mech. Eng. Press. Vessels Pip. Div. Publ. PVP*, vol. 3, 2012.

[7] C. Zigh y J. Solis, «Computational Fluid Dynamics Best Practice Guidelines for Dry Cask Applications Final Report», 2013.

[8] J. Li y Y. Y. Liu, «Thermal modeling of a vertical dry storage cask for used nuclear fuel», *Nucl. Eng. Des.*, vol. 301, n.º March, pp. 74–88, 2016.

[9] EPRI, *The TN-24P PWR Spent-Fuel Storage Cask: Testing and Analyses*. 1987.

[10] S. H. Yoo, H. C. No, H. M. Kim, y E. H. Lee, «CFD-assisted scaling methodology and thermal-hydraulic experiment for a single spent fuel assembly», *Nucl. Eng. Des.*, vol. 240, n.º 12, pp. 4008–4020, 2010.

[11] T. L. Bergman y F. P. Incropera, Eds., *Fundamentals of heat and mass transfer*, 7th ed. Hoboken, NJ: Wiley, 2011.

[12] P. J. Roache, «Quantification of Uncertainty in Computational Fluid Dynamics», *Annu. Rev. Fluid Mech.*, vol. 29, n.º 1, pp. 123–160, 1997.

[13] P. J. Roache, «Verification and Validation in Computational Science and Engineering», *Comput. Sci. Eng.*, pp. 8–9, 1998.